Efficiently enhancing the photocatalytic activity of g-C_3N_4 by a simple advanced successive activation method

Xu Huai[1], Zusheng Hang[1,2], Zhangzhong Wang[1,2] ✉, Delin Liu[1], Qiuya Li[1], Zhen He[1], Yang Chen[1], Xisi Han[1]

[1]*School of Materials Science and Engineering, Nanjing Institute of Technology, Nanjing 211167, People's Republic of China*
[2]*Jiangsu Key Laboratory of Advanced Structural Materials and Application Technology, Nanjing 211167, People's Republic of China*
✉ *E-mail: zzww@njit.edu.cn*

Published in Micro & Nano Letters; Received on 18th July 2017; Revised on 28th August 2017; Accepted on 5th December 2017

High activated graphitic carbon nitride (g-C_3N_4) was initially produced by a typical calcination of melamine, and then modified by a convenient successive activation: protonated in hydrothermal hydrochloric acid (g-C_3N_4-1) and subsequently immersed in aqueous sodium hydroxide solution (g-C_3N_4-2). Scanning electron microscopy (SEM), transmission electron microscopy (TEM), X-ray diffraction (XRD) and thermogravimetry were used to characterise the morphology, crystal structure and thermal stability of the as-prepared samples. The SEM and TEM showed that g-C_3N_4-2 had a much smaller aggregate size than g-C_3N_4-1 and obviously displayed porous structures. The XRD patterns indicated the decrease of inter-lamellar spacing between the layers of samples and the increase of stretched properties of g-C_3N_4-2. Under visible-light irradiation, the modified g-C_3N_4 showed higher photocatalytic activity for degradation of rhodamine B solution than pristine samples due to the tiny particles aggregate and porous structure. Thus, the method of acid and alkali treatment will widen the photocatalysis and application of g-C_3N_4.

1. Introduction: Graphitic carbon nitride (g-C_3N_4) with a visible-light-driven bandgap and proper band edges presents a great prospect in catalysis [1, 2], pharmaceutics [3] and energy [4]. It was discovered that g-C_3N_4 can catalyse the decomposition of water [5, 6], organic pollutants [7], heavy metal ions [8] and so on. Since then, this excellent stable and metal-free material has been extensively studied for its emerging photocatalytic degradation of organic pollutants [9, 10].

Some investigations reported that the photocatalytic performance of pure g-C_3N_4 can be enhanced by activation with acid. For instance, Zhang *et al.* [11] investigated that g-C_3N_4 could be reversibly protonated by strong mineral acids, resulting in an enhanced solubility, dispersability, electronic structure, and surface area. Moreover, Li *et al.* [12] used the method of chemical oxidation with $K_2Cr_2O_7$–H_2SO_4 to enhance the photocatalytic activity of bulk g-C_3N_4 towards rhodamine B (RhB) photodegradation. Meanwhile, the activation of g-C_3N_4 by sole alkaline method was also reported. For example, Zhang *et al.* [13] obtained the modified g-C_3N_4 via treatment in 0.2 mol/L NaOH aqueous solution at 80°C for 6 h. In the presence of the alkali treated g-C_3N_4, the reduced ratio of Cr^{6+} was >95% when irradiated by visible-light for 120 min. Through these studies, it was found that the photocatalytic activity could be improved by activation method. However, these researches mainly focus on single activation of acid or alkaline method, respectively. It is widely accepted to date that the strategy of acid activation is ascribed to the tri-*s*-triazine units connected by amino groups in each layer [14]. The acid activation of g-C_3N_4 would result in the formation of new acid sites on its surface [14]. Then, based on the acid–base reaction principle, it is easily considered that the acidified g-C_3N_4 will be conducive to the further activation with alkaline solution to endow with better photocatalytic performance [15]. Additionally, the activation methods to photocatalytic activity of g-C_3N_4 do require targeted improvements.

In this Letter, we successively activated g-C_3N_4 by hydrochloric acid protonation and then alkaline hydrothermal treatment. The micromorphology, crystal structure, thermal stability and photocatalytic activity of the resultant samples were characterised. What the most important is that, compared to single activated products, the treated g-C_3N_4 with this simple advanced successive activation is more efficient in photocatalytic activity towards degradation of RhB solution.

2. Experimental details: All chemicals were reagent grade and not further purified. To produce pure g-C_3N_4, 30 g of melamine in a muffle furnace is heated at 773 K for 1 h, ramped at a rate of 10 K min^{-1} and then heated at 823 K for 1 h. The product was collected and ground into powder.

Activated g-C_3N_4 was synthesised via two steps. First was to mixed 1 g pure g-C_3N_4 powder with 5 .9 mol L^{-1} HCl and ultrasonicate for 10 min. at room temperature. The treated mixture was slowly pulled into 100 mL hydrothermal reaction vessel for 2 h at 373 K, and then filtered, washed, and dried overnight. The acidified g-C_3N_4 was obtained in advance, which was named as g-C_3N_4-1. Secondly, a 0.2 g g-C_3N_4-1 was added to 0.2 mol L^{-1} NaOH by sonication for 10 min. and then pulled into the same hydrothermal reaction vessel for 2 h at 373 K, and then filtered, washed, and dried. After the processes, a subsequent alkali-treated g-C_3N_4 was obtained, which was named as g-C_3N_4-2. Applying this successive activation route can successfully produce the exfoliated and highly efficient photocatalytic g-C_3N_4-2.

SEM and TEM images were, respectively, taken on Merlin Compact microscope (Carl Zeiss, Germany) and Tecnai 12 instrument (FEI, USA). The phase identification of prepared samples was characterised by X-ray diffraction (XRD) on a UltimaIV diffractometer (Rigaku Corporation, Japan). Thermogravimetry (TG) was recorded on an HTG-1 instrument (Beijing Henven Experimental Equipment Co., Ltd. China). Evaluated by the degradation of RhB solution (5 mg L^{-1}, 100 mL) and described elsewhere [16], the photocatalytic activity of products was characterised under visible light irradiation using a 1000 W xenon lamp (LXHL-LR3C, Shanghai) with a 420 nm cutoff filter as the light source, with the addition of 0.2 mL hydrogen peroxide as sacrificial reagent. Prior to irradiation, the RhB solution containing resultant samples was magnetically stirred for 60 min in the dark to reach

© The Institution of Engineering and Technology 2017

the absorption–desorption equilibrium. The suspension was collected at an interval of 10 min and detected.

3. Results and discussion: Fig. 1 displays SEM (a–c) and TEM (d–f) images of pure g-C_3N_4 (a and d), g-C_3N_4-1 (b and e) and g-C_3N_4-2 (c and f). Observed from Figs. 1*a*–*c*, it can be seen all products have a typical stacked structure, and the aggregate sizes become increasingly smaller with the process of activation. Obviously, the evolution of the morphology from bulk structures to small size particles is along with the chemical reaction process, which leads to the different types of sheet stacking structures between pure and modified g-C_3N_4 [17]. It also implies that the chemical activation process of subsequent alkali treatment is of high efficiency due to the well-acidified pretreatment of g-C_3N_4-1. The TEM pictures show that the g-C_3N_4-2 displaying similar layered appearance as g-C_3N_4-1 obviously possesses numbers of pores. This suggests that during the further activation by NaOH, the plane sizes of g-C_3N_4-2 are converted into smaller than that of acidified g-C_3N_4-1. These results also indicate that many small fragments are exfoliated and peeled off g-C_3N_4-1 [18].

The XRD patterns of pure g-C_3N_4, g-C_3N_4-1 and g-C_3N_4-2 are recorded in Fig. 2. It is known that the low reflection peak (100) reflects the in-plane structural repeating motifs, such as the hole-to-hole distance, while the high-angle peak (002) is related to the characteristic interlayer stacking reflections of the aromatic systems [12, 19]. The nearly same XRD patterns in Fig. 2 suggest that the tectonic units of tri-*s*-triazine ring and the intrinsic crystal structure of g-C_3N_4 have been maintained [20]. With respect to pure g-C_3N_4, the (100) peak for the lattice planes of g-C_3N_4-1 becomes less pronounced and shifts from 13.12° to 12.90°. After alkali modification, it turns sharp and shifts to a lower angle of 12.22, indicating the decrease of plane size and the increasingly stretched properties of g-C_3N_4-2 [21]. Moreover, the strong XRD peak (002) of g-C_3N_4-1 and g-C_3N_4-2 are both slightly broadened

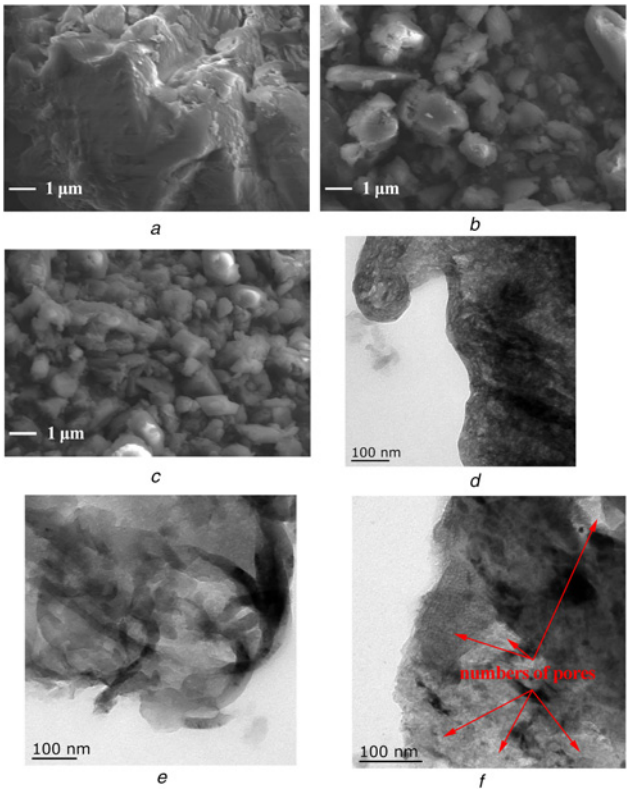

Fig. 1 *Scanning electron micrographs*
a Pure g-C_3N_4
b g-C_3N_4-1
c g-C_3N_4-2
And TEM
d pure g-C_3N_4
e g-C_3N_4-1
f g-C_3N_4-2

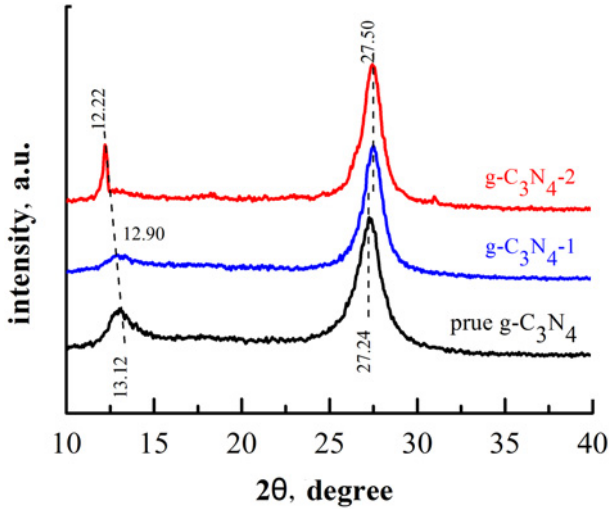

Fig. 2 *XRD patterns of pure g-C_3N_4, g-C_3N_4-1 and g-C_3N_4-2*

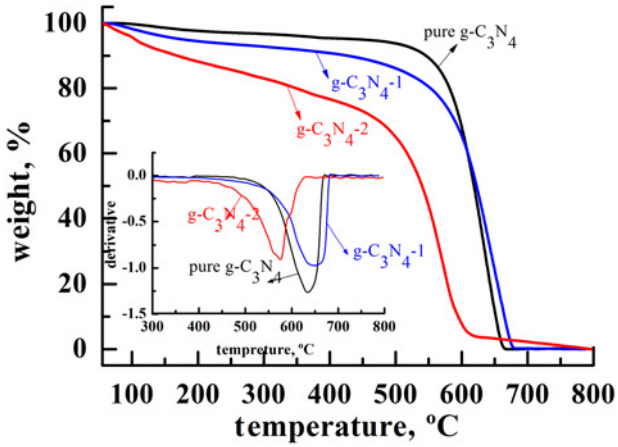

Fig. 3 *TG and DTG images of pure g-C_3N_4, g-C_3N_4-1 and g-C_3N_4-2*

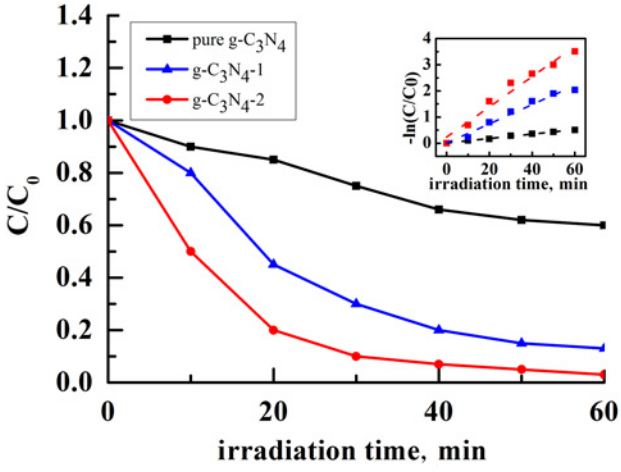

Fig. 4 *Photocatalytic degradation of RhB over pure g-C_3N_4, g-C_3N_4-1 and g-C_3N_4-2 under visible light irradiation*

© The Institution of Engineering and Technology 2017

doi: 10.1049/mnl.2017.0518

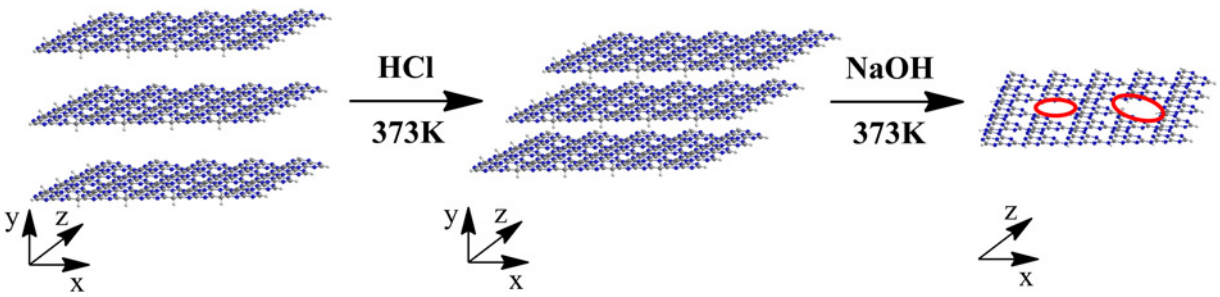

Fig. 5 *Schematic activation process of g-C_3N_4 in HCl and subsequent NaOH solution*

and shift from 27.24° to 27.50°, which indicates a slight decreased inter-lamellar spacing and gallery distance between the layers of samples [12, 21]. We can correspondingly see from the SEM images that it is related to the micro-structure reformation with the activation proceeding. These results can be explained by the interaction among the tri-*s*-triazine units of g-C_3N_4, hydrogen chloride and sodium hydroxide solution [21], which is detailly explanted in the discussion of proposed mechanism.

Fig. 3 shows the TG curves (insert presents the DTG curves) of g-C_3N_4 before and after activation. As the temperature increases, the g-C_3N_4-2 shows faster weight loss state than pure g-C_3N_4 and g-C_3N_4-1 from the ambient temperature to 450°C. This weight loss is attributed to dehydration, ammonia and decomposition of the labile functional groups in the activated carbon nitride networks.

The inserted DTG curve shows another huge loss of g-C_3N_4-2 starts from 450°C with a sharp endothermic peak at 570°C and residually decomposes to 5% at 600°C, illustrating a little lower thermal stability than pure g-C_3N_4 and g-C_3N_4-1. The exothermic peak and completely decomposed temperature of g-C_3N_4-1 are, respectively, at about 650°C and 680°C, which was 20°C higher than that of pure g-C_3N_4. It is possible that the different morphology and structure are reformed after the successive activation treatments. Meanwhile, the thermal stability seemed to be weakly poor with the proceeding of activation strategy due to the partial exfoliation of bulk g-C_3N_4 and the fabrication of porous structure.

Fig. 4 displays photocatalytic activity of pure g-C_3N_4, g-C_3N_4-1 and g-C_3N_4-2 (insert presents the dynamical fitting curves of reaction kinetics of photocatalytic degradation). In general, the concentration of RhB for all the samples gradually decreases with increasing visible light irradiation time. Additionally, the photocatalytic performance of RhB degradation enhance with the activated procedure of g-C_3N_4 samples. Especially, the absorbance of RhB decreases sharply in the presence of g-C_3N_4-2 and mostly disappears within 30 min. It indicates that g-C_3N_4-2 exhibits the highest activity for the photodegradation of RhB under visible light irradiation among the samples.

From the insert of Fig. 4, the slope (k) of dynamic equation ($-\ln(C/C_0)=kt$) is positively correlated with the photocatalytic activity, so it is especially pronounced that the order of photocatalytic activity is g-C_3N_4-2 > g-C_3N_4-1 > pure g-C_3N_4. In detail, the photocatalytic activity of g-C_3N_4-2 is calculated average about 6.8 higher than that of pure g-C_3N_4. Based on all above discussion, including micromorphology, crystal structure as well as thermal stability, it is well considered that the increase of photocatalytic efficiency benefits from the change of morphology, the tiny particles aggregate and the fabrication of porous structure.

The proposed mechanism for successive activation of g-C_3N_4 is presented in Fig. 5. As a polymer sheet constituted with tri-*s*-triazine, each layer of g-C_3N_4 is regarded as a multistage polymerised weak base. The introduction of hydrothermal hydrochloric acid forms a hydrogen chloride intercalated complex, which draws the interlayer distances closer [21]. This result is in good agreement with the shift of the high-angle peak in XRD patterns. Simultaneously, it turns foreseeable for exfoliation and slip to decrease the aggregate size. Afterward, the immersion in NaOH solution at 373 K facilitates the partial hydrolysis of C–NH–C bonds between bridge nitrogen atoms and tri-*s*-triazine units, which results in the further split of g-C_3N_4-1 polymer chains. Consequently, the unstable domains contain in g-C_3N_4-1 are preferentially decomposed into fragments and relatively stable domains of porous g-C_3N_4-2 particles [22], which can be obviously seen from the morphology of SEM/TEM images and the decreasing shift of low reflection peak in XRD results.

4. Conclusion: In summary, we reported a simple advanced successive activation method, acidification and subsequent alkaline treatment, to modify g-C_3N_4 for enhancing its photocatalytic activity. Thanks to the interaction among the tri-*s*-triazine units of g-C_3N_4, hydrogen chloride and sodium hydroxide solution, many small fragments are exfoliated and peeled off the g-C_3N_4-1. Consequently, there is a decrease of inter-lamellar spacing between the layers of samples, a decrease of aggregate and plane size, an increase of stretched properties of g-C_3N_4-2. Benefited from the change of morphology and porous structures of g-C_3N_4-2, it exhibits a high photocatalytic activity under visible light irradiation, averagely about 6.8 higher than that of pure g-C_3N_4. It is a pity that the thermal stability of g-C_3N_4-2 is relatively low when sharply decomposed at 570°C, but it does not affect its service performance under normal temperature. Predictably, our study will provide new insight into the photocatalysis and application of g-C_3N_4.

5. Acknowledgments: This work was supported by the Natural Science Foundation of Jiangsu Province (grant no. BK20130747), Jiangsu Province Science and Technology Support Program (grant no. BE2014039), Jiangsu Key Laboratory Opening Project of Advanced Structural Materials and Application Technology (grant no. ASMA201505), the Research Innovation Program for College Graduates of Jiangsu Province (grant no. SJLX16_0663), the Practice and Innovation Training Program Projects for Jiangsu College Students (grant no. 201711276008Z) and the Students' Science and Technology Innovation Fund Project of Nanjing Institute of Technology (grant nos. TP20160201, TZ20161701, TB201702005).

6 References

[1] Niu P., Zhang L., Liu G., *ET AL.*: 'Graphene-like carbon nitride nanosheets for improved photocatalytic activities', *Adv. Funct. Mater.*, 2012, **22**, (22), pp. 4763–4770

[2] Tan L., Xu J., Zhang X., *ET AL.*: 'Synthesis of g-C_3N_4/CeO_2 nanocomposites with improved catalytic activity on the thermal decomposition of ammonium perchlorate', *Appl. Surf. Sci.*, 2015, **356**, pp. 447–453

[3] Liao X., Wang Q., Ju H.: 'A peptide nucleic acid-functionalized carbon nitride nanosheet as a probe for in situ monitoring of intracellular microrna', *Analyst*, 2015, **140**, (12), pp. 4245–4252

[4] Byon H.R., Suntivich J., Shao-Horn Y.: 'Graphene-based non-noble-metal catalysts for oxygen reduction reaction in acid', *Chem. Mater.*, 2011, **23**, (23), pp. 3421–3428

© The Institution of Engineering and Technology 2017

[5] Wang X., Maeda K., Thomas A., *ET AL.*: 'A metal-free polymeric photocatalyst for hydrogen production from water under visible light', *Nat. Mater*, 2009, **8**, (1), pp. 76–80
[6] Dong G., Zhang Y., Pan Q., *ET AL.*: 'A fantastic graphitic carbon nitride (g-C_3N_4) material: electronic structure, photocatalytic and photoelectronic properties', *J. Photochem. Photobiol. C, Photochem. Rev.*, 2014, **20**, pp. 33–50
[7] Cui Y., Ding Z., Liu P., *ET AL.*: 'Metal-free activation of H_2O_2 by g-C_3N_4 under visible light irradiation for the degradation of organic pollutants', *Phys. Chem. Chem. Phys.*, 2012, **14**, (4), pp. 1455–1462
[8] Shen C., Chen C., Wen T., *ET AL.*: 'Superior adsorption capacity of g-C_3N_4 for heavy metal ions from aqueous solutions', *J. Colloid Interface Sci.*, 2015, **456**, pp. 7–14
[9] Yu Q., Guo S., Li X., *ET AL.*: 'One step fabrication and high photocatalytic activity of porous graphitic carbon nitride/graphene oxide hybrid by direct polymerization of cyanamide without templates', *Micro Nano Lett.*, 2014, **88**, (10), pp. 1643–1649
[10] Zhang J., Chen Y., Wang X.: 'Two-dimensional covalent carbon nitride nanosheets: synthesis, functionalization, and applications', *Energy Environ. Sci.*, 2015, **8**, (11), pp. 3092–3108
[11] Zhang Y., Thomas A., Antonietti M., *ET AL.*: 'Activation of carbon nitride solids by protonation: morphology changes, enhanced ionic conductivity, and photoconduction experiments', *J. Am. Chem. Soc.*, 2009, **131**, (1), pp. 50–51
[12] Li H.-J., Sun B.-W., Sui L., *ET AL.*: 'Preparation of water-dispersible porous g-C_3N_4 with improved photocatalytic activity by chemical oxidation', *Phys. Chem. Chem. Phys.*, 2015, **17**, (5), pp. 3309–3315
[13] Zhang Q., Liu S., Zhang Y., *ET AL.*: 'Enhancement of the photocatalytic activity of g-C_3N_4 via treatment in dilute NaOH aqueous solution', *Mater. Lett.*, 2016, **171**, pp. 79–82
[14] Zhang L., Liu D., Guan J., *ET AL.*: 'Metal-Free g-C_3N_4 photocatalyst by sulfuric acid activation for selective aerobic oxidation of benzyl alcohol under visible light', *Mater. Res. Bull.*, 2014, **59**, pp. 84–92
[15] Cai J., Bennici S., Shen J., *ET AL.*: 'The acid-base properties of nitrogen-containing mesoporous carbon materials', *Microporous Mesoporous Mater.*, 2015, **212**, pp. 156–168
[16] Bhandary N., Singh A.P., Kumar S., *ET AL.*: 'In situ solid-state synthesis of a AgNi/g-C_3N_4 nanocomposite for enhanced photoelectrochemical and photocatalytic activity', *ChemSusChem*, 2016, **9**, (19), pp. 2816–2823
[17] Zhang Y., Pan Q., Chai G., *ET AL.*: 'Synthesis and luminescence mechanism of multicolor-emitting g-C_3N_4 nanopowders by low temperature thermal condensation of melamine', *Sci. Rep.*, 2013, **3**, (1), pp. 1943–1950
[18] Cheng F., Yan J., Zhou C., *ET AL.*: 'An alkali treating strategy for the colloidization of graphitic carbon nitride and its excellent photocatalytic performance', *J. Colloid Interface Sci.*, 2016, **468**, pp. 103–109
[19] Zhang J., Zhang M., Lin L., *ET AL.*: 'Sol processing of conjugated carbon nitride powders for thin-film fabrication', *Angew. Chem. Int. Ed.*, 2015, **54**, (21), pp. 6297–6301
[20] Guo Q., Zhang Y., Qiu J., *ET AL.*: 'Engineering the electronic structure and optical properties of in-situ solid-state synthesis of a AgNi/g-C_3N_4 nanocomposite for enhanced photoelectrochemical and photocatalytic activity by non-metal ion doping', *J. Mater. Chem. C*, 2016, **4**, (28), pp. 6839–6847
[21] Du X., Zou G., Wang Z., *ET AL.*: 'A scalable chemical route to soluble acidified graphitic carbon nitride: an ideal precursor for isolated ultrathin G-C_3n_4 nanosheets', *Nanoscale*, 2015, **7**, (19), pp. 8701–8706
[22] Sano T., Tsutsui S., Koike K., *ET AL.*: 'Activation of graphitic carbon nitride (g-C_3N_4) by alkaline hydrothermal treatment for photocatalytic no oxidation in gas phase', *J. Mater. Chem. A*, 2013, **1**, (21), pp. 6489–6496

© The Institution of Engineering and Technology 2017

doi: 10.1049/mnl.2017.0518